

Mechanically Generated Surface Chirality at the Nanoscale

Sameh Ferjani,¹ Yoonseuk Choi,^{1,2} Joel Pendery,¹ Rolfe G. Petschek,¹ and Charles Rosenblatt¹

¹*Department of Physics, Case Western Reserve University, Cleveland, Ohio 44106-7079, USA*

²*Department of Electrical Engineering, Hanbat National University, Daejeon, Korea 305-719*

(Received 15 December 2009; revised manuscript received 27 May 2010; published 24 June 2010)

A substrate coated with an achiral polyimide alignment layer was scribed bidirectionally with the stylus of an atomic force microscope to create an easy axis for liquid crystal orientation. The resulting noncentrosymmetric topography resulted in a chiral surface that manifests itself at the molecular level. To show this unambiguously, a planar-aligned negative dielectric anisotropy achiral nematic liquid crystal was placed in contact with the surface and subjected to an electric field E . The nematic director was found to undergo an azimuthal rotation approximately linear in E . This so-called “surface electroclinic effect” is a signature of surface chirality and was not observed when the polyimide was treated for a centrosymmetric topography, and therefore was nonchiral.

DOI: 10.1103/PhysRevLett.104.257801

PACS numbers: 61.30.Hn

Chirality plays a central role in both large scale and small scale systems. On large scales, technologies such as the mechanical screw date back to antiquity. On microscopic and nanoscopic scales, chirality plays a central role in physics and biology, and is crucial for the existence of life. Most often macroscopic consequences of chirality, such as optical rotatory power in a bulk material, occur as a result of the absence of inversion symmetry of the constituent components, such as molecules or self-assembled structures. But this is not a requirement for bulk chirality. In fact, achiral molecules have been shown to self-organize into macroscopically chiral phases [1–3], which can occur at interfaces due to the specifics of the molecule-substrate interactions. Chiral molecules such as DNA also have been used as templates to induce chirality in inherently achiral materials [4,5]. In this Letter we demonstrate nanoscale mechanical generation of chirality along a corrugated surface of molecular thickness by nano-scribing, where surface chirality is defined as the inability to superpose an object onto its mirror image by rotation and translation; this corresponds to the absence of *any* mirror plane that includes the average surface normal. The letter F is surface chiral, whereas the letter E is achiral. Chiral surface patterns such as a multiturn or multiarm spiral (similar to certain spiral galaxies or an Eastern religious symbol) have been created by several techniques, such as lithography [6] and vacuum evaporation [7]. These tend to have large length scales, however, typically several to hundreds of micrometers. Glancing angle deposition has been used to create thin ($\geq 1 \mu\text{m}$)—albeit three-dimensional—arrays of chiral screwlike structures of SiO, CaF₂ and other materials [8]. In a recent paper we examined bidirectional scribing of an inherently achiral polymer-coated substrate using the stylus of an atomic force microscope (AFM) [9]. The sequential “pulling” and “pushing” actions of the AFM stylus and the resulting transport of material resulted in a noncentrosymmetric topography, and thus a noncentrosymmetric interaction

potential with the adjacent liquid crystal (LC). We conjectured that the resulting topographically noncentrosymmetric axis, which is perpendicular to the scribing axis, and the scribing axis itself form a two-dimensional basis (like the number “7”) that lacks mirror symmetry on the surface. When coated with a nematic LC, the LC displayed a striped optical texture. But when the substrate was scribed unidirectionally, resulting in a centrosymmetric topography, stripes were not observed. One possible explanation is the generation of surface chirality. Nevertheless, several other phenomena also could have been responsible for the stripes, such as coupling between splay elasticity and a soft mode [10,11] or saddle-splay elasticity [12–14]. In this Letter we conclusively demonstrate nanoscopic scribing-induced chirality at a polymer surface by detecting a small electric field-induced rotation of an achiral nematic LC adjacent to the surface. The magnitude of this rotation, moreover, provides a sensitive measure of the relative strength of the induced chirality. An ability to control the sign and strength of the chirality on nanoscopic length scales is of broad interest. For example, as optical sensors for (chiral) biological molecules, to control nucleation and growth of chiral self-assemblies from achiral precursors, and to facilitate resolution of mixtures of enantiomers by local control of nucleation [2,15,16]. Although at present the magnitude of such effects are a matter of speculation, we will suggest a number of scribing patterns that may be useful to enhance the response.

Meyer and Garoff demonstrated [17] an “electroclinic effect” (ECE) in the bulk smectic- A phase of a chiral LC, whereby an electric field applied parallel to the smectic layers induces a rotation of the LC director about the electric field axis. This effect requires the absence of mirror symmetry in the LC molecules. Li, *et al.* observed a related bulk nematic ECE [18,19] due to the presence of smectic fluctuations in a chiral nematic phase. Chirality-based phenomena at LC/substrate interfaces also have been well-studied, including numerous reports of layer tilt in the

chiral smectic-A phase at a rubbed surface [20–23]. Polymerizable chiral smectic- C^* LCs have been used as fixed pretilt alignment layers; an applied field reorients the smectic- C^* surface layer, which then couples elastically to the bulk LC [24,25]. Tripathi, *et al.* observed a linear electrooptic effect [26]—in essence, a type of ECE—at the interface between an achiral substrate and a chiral nematic LC. More recently it was shown that an *achiral* nematic tilts by an angle β with respect to the rubbing direction at a molecularly *chiral* alignment layer [27,28]. This effect arises from the biased molecular rotation and resulting polarization at, and normal to, the interface. If the surface is achiral the tilt can be either clockwise or counter-clockwise with equal probability, resulting in zero net tilt; if the surface is chiral, one tilt direction is preferred and a net tilt occurs, although its magnitude depends on the LC, the alignment layer, and the degree of chiral coupling. Moreover, application of an electric field normal to the surface would couple to the polarization and modify the tilt—again, this is one manifestation of the ECE. The ingredient required for all of these tilt phenomena is the breaking of mirror symmetry. Thus, the observation of a LC electroclinic effect at the interface would serve as a sensitive proof of mechanically generated chirality at the surface.

A pair of glass substrates coated with a semitransparent layer of indium-tin-oxide (ITO) was cleaned sequentially in detergent, acetone, and ethanol. One substrate was spin coated for 20 s at 2000 rpm with a layer of the polyamic acid RN-1175 (Nissan Chemical Industries), then imidized by baking according to the manufacturer’s specifications at 250 °C for 60 min. The thickness of the alignment layer t_A was measured by a mechanical profilometer and found to be $t_A = 200 \pm 20$ nm. Several squares of size $100 \times 100 \mu\text{m}$ were scribed into the polyimide surface by the stylus (TAP-300 Si) of a Topometrix Explorer AFM. Two different patterns were scribed several times each, in close proximity to each other: A bidirectional pattern involved translating the stylus back and forth (i.e., pulling and pushing) at an angle $\theta = 60^\circ$ with respect to the cantilever orientation, as shown in Fig. 1(a). We remark that the details of the scribed pattern must be on length scales comparable to, or smaller than, the LC’s extrapolation length L , which corresponds to a characteristic distance over which the nematic director remains correlated in the presence of spatial variations in the surface patterning [29]. The quantity $L = K/W_2$, where K is an appropriate elastic modulus and W_2 is the spatially averaged quadratic coefficient for the surface free energy expanded in powers of the angular deviation from the scribed axis [30]. The magnitude of L typically is many hundreds of nanometers for strong scribing (large W_2) and $1 \mu\text{m}$ or more for weak scribing forces [31]. Given this condition, we chose a $d = 200$ nm spacing between adjacent lines, although more closely spaced lines easily are possible [31,32]. Figure 1(c) shows the cross-sectional topography obtained in noncontact AFM mode, which clearly is noncentrosym-

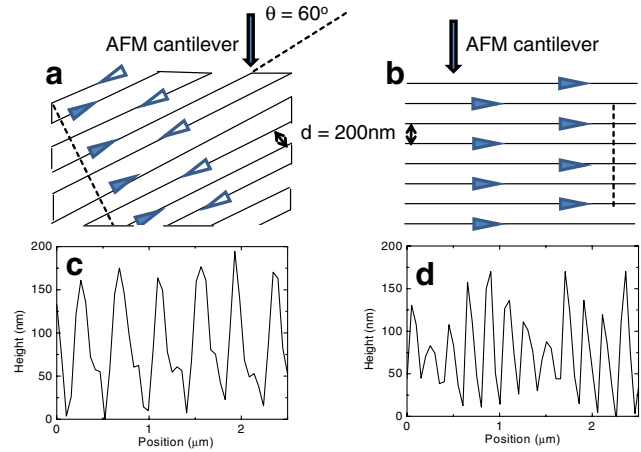


FIG. 1 (color online). Patterns for (a) bidirectional and (b) unidirectional scribing. The orientation of the AFM cantilever is shown. Panel (c) shows a typical topographical profile [along the dashed line in panel (a)] for the bidirectional scribing, and panel (d) shows a typical topographical profile [along the dashed line in panel (b)] for the unidirectional scribing.

metric. By itself the topography in Fig. 1(c) is not chiral, although one can associate a vector with the topography’s gradient within each repeat period. Additionally, since pulling and pushing are different actions, there is a vector associated with the AFM-created troughs that depends in part on the angle that the pushing and pulling directions make with the cantilever. It is the *combination* of these vectors that results in a chiral surface, irrespective of the presence of a LC, and it is the goal of this work to confirm this conjecture. To accomplish this, we note that because of this supposed chirality, the nematic molecules must azimuthally rotate slightly about the scribing axis, resulting in an additional biasing of the molecular rotation about its long axis. Application of an electric field modifies this rotational biasing, causing a small change in the molecules’ azimuthal orientation, which we measure optically. On the other hand, the unidirectional pattern [Fig. 1(b)] has on average a centrosymmetric cross-sectional topography [Fig. 1(d)]. Because this has a C_2 rotation about an axis normal to the surface (unlike a vector), its surface must be achiral. As an aside, we note that in addition to the azimuthal director deviation from the scribing axis, the topography results in a polar director pretilt of $\sim 1^\circ$ for bidirectional scribing (and larger for unidirectional scribing) [33], which gives an orientationally, and perhaps even a translationally, 3D character to the chirality induced in the LC. Nevertheless, neither the surface chirality of the alignment layer nor the induction of chirality in the LC requires a LC director component along the average surface normal. In fact, our surface also may result in a chiral director pattern in the plane perpendicular to the average surface normal. The opposing substrate was spin coated with polymethylmethacrylate (PMMA) dissolved in 66% vol. propylene glycol methyl ether acetate with 33% vol. γ -butyrolacetone and baked at 80 °C for 120 min. The

thickness t_{PMMA} of the PMMA layer was measured to be $\sim 1000 \mu\text{m}$. The PMMA provides a planar-degenerate surface for alignment of the LC, where the azimuthal orientation at the PMMA “slave” surface is controlled initially by the RN-1175 coated “master” surface [34]. Over several hours a memory effect [35] develops at the PMMA substrate, and the initial orientation of the LC becomes fixed at that substrate. The two substrates were placed together, separated by Mylar spacers, and cemented. The thickness $t_{\text{LC}} = 6.0 \pm 0.1 \mu\text{m}$ of the gap between the alignment layers was measured by interferometry. After attaching wires to the ITO electrodes, the cell was filled with the negative dielectric anisotropy and low resistivity LC methoxybenzylidene butylaniline (MBBA) in its isotropic phase at a temperature 53°C . The cell then was cooled into the nematic phase and stabilized at room temperature, approximately 22°C . We note that the deviation angle β of the director at the supposedly chiral surface was too small to detect— β was well under 1° —indicating weak coupling to the chirality.

Now let us consider the application of a low frequency ($f = 2 \text{ Hz}$) voltage across the cell, which reached as high as $V_{\text{app}} = 145 \text{ V}$. If an ECE were present at the presumed chiral surface, the director would undergo a small twist from the fixed PMMA substrate to the chiral RN-1175 substrate. The low frequency was used to ensure that the director profile would follow the ac voltage adiabatically. Ordinarily, a negative anisotropy LC such as MBBA would exhibit an instability at low frequencies at a relatively small voltage [29]; this was not observed, however. The reason is that at low frequencies the two alignment layers and the LC layer act as resistors, rather than capacitors, in series. To determine the effective voltage drop V_{LC} across the LC layer we constructed another cell having the same gap t_{LC} but without the alignment layers and filled it with MBBA, which in this cell was in direct contact with the ITO. Using an electrometer, we measured the dc resistance across the MBBA-only cell and the cell having the two alignment layers, finding resistances of $1.4 \times 10^6 \Omega$ and $4 \times 10^8 \Omega$, respectively. Thus the voltage drop across the LC was much smaller than that across the alignment layers ($V_{\text{LC}} \approx 0.0035V_{\text{app}}$), insufficient to induce the instability.

The optical setup consisted of a beam from a Nd-YaG laser at wavelength 532 nm that passed through a polarizer, through the sample with the PMMA side facing the laser, a second polarizer oriented at 45° with respect to the first polarizer, a microscope lens to create an enlarged real image (magnification $\sim 20X$) of the LC sample downstream, a $500 \mu\text{m}$ diameter pinhole, and into a photodiode detector. The detector output was fed into a lock-in amplifier operating in amplitude or phase (R/θ) mode and referenced to V_{app} . The signal from the lock-in amplifier (1 s time constant filter) was computer recorded. The MBBA cell was oriented so that the director was parallel to the initial polarizer. (Because the unidirectional and bidirectional axis orientations were different, the cell had

to be rotated when examining the two different surface scriptions.) We chose this optical configuration to exclude an undesired consequence of a coupling between the applied field and the two surface polarizations: If we had used crossed polarizers with the LC director at 45° with respect to the two polarizers, the voltage-induced variation of the MBBA orientational order parameter at the two dissimilar surfaces would have resulted in a variation at frequency f of the optical retardation through the cell, and thus the intensity at the detector [36–38]. Our geometry excludes this effect because, even though the MBBA order parameter at the surfaces can vary slightly with applied field, only the extraordinary optical mode propagates through the cell and thus the resulting signal is insensitive to changes in retardation. But, if the azimuthal orientation α of the director at the supposedly chiral surface were to vary with the applied voltage, as it should on symmetry grounds, the director would undergo a small twist from its perturbed orientation at the chiral scribed substrate to its (nearly) pinned orientation at the PMMA substrate. The optical polarization would adiabatically rotate through the cell and the resulting intensity of light passing through the second polarizer would vary approximately linearly with $\delta\alpha$ at frequency f . This is the signal that we observe.

The voltage V_{app} applied to the cell was increased from zero to 145 V rms in steps of 0.65 V , with a dwell time $\tau = 10 \text{ s}$ at each step. Figure 2(a) shows a typical result for the bidirectionally scribed surface: field-induced tilt $\delta\alpha$ vs V_{app} along the lower axis, with the voltage drop V_{LC} across the LC shown along the upper axis. The azimuthal deviation $\delta\alpha$ was obtained from the intensity data by noting that, neglecting reflections, the intensity $I = I_0 \cos^2(\frac{\pi}{4} + \delta\alpha)$, where I_0 is the incident intensity of light. For small $\delta\alpha$, $I \approx I_0(\frac{1}{2} - \delta\alpha)$. Thus, the ratio of the ac signal at frequency f to the dc signal corresponds to

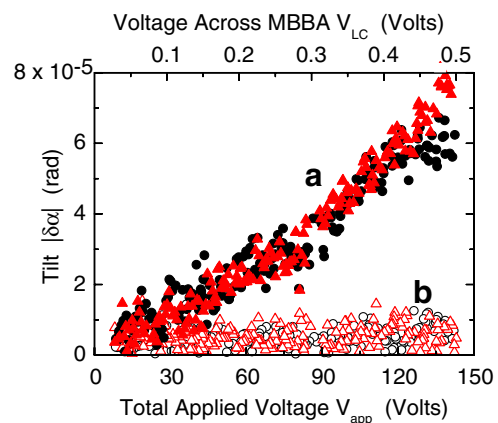


FIG. 2 (color online). Experimental results for bidirectionally scribed 2D chiral surface (solid symbols) and for unidirectionally scribed achiral surface (open symbols). Note that the signal does not vanish at zero voltage, as the lock-in amplifier was operated in R/θ mode. Circles (black) correspond to data on increasing the voltage with time, and triangles (red) correspond to decreasing the voltage with time. No hysteresis was observed.

$-2\delta\alpha$. Experiments were performed at several bidirectionally scribed squares, with similar qualitative results. We note, however, that the slope could vary by more than a factor of 2 from one run to the next, indicative of variations in the strength of the chiral environment due to experimental inconsistencies in the scribing process. We then examined the unidirectionally scribed squares that exhibit a centrosymmetric topography; these squares are not expected to be chiral. Figure 2(b) shows a typical result. Notice that there is no systematic variation in the signal at frequency f , indicating the absence of an ECE. This null result indicates that even though the polar and azimuthal “pretilts” could affect the magnitude of the ECE for the bidirectionally scribed surface, the ECE could not exist if the main ingredients of the surface chirality (the scribing vector and noncentrosymmetry vector) were absent.

The appearance of an electroclinic effect at the bidirectionally scribed surface and its absence at the unidirectionally scribed surface is an unambiguous signature of mechanically generated chirality at the bidirectionally-scribed surface. To be sure, the demonstrated effect is small. Nevertheless, that this chirality manifests itself at the molecular level suggests other patterns such as dividing a region into subregions, each with uniform scribing but with an overall nonzero curl [39], imprinting a grid of parallelograms [40], unidirectional scribing with forces varying sequentially as $ABCABCABC\dots$; or scribing steplike patterns. These may provide a significantly larger response at the molecular scale.

The authors thank R. Lemieux, J. Vij, G. Carbone, H. Yokoyama, K. Kash, and T. J. Atherton for useful discussions. C. R. and Y. C. were supported by the Department of Energy’s Office of Science under grant DE-FG02-01ER45934, S.F. by the NSF under grant DMR-0804111, J. P. by the Department of Education’s GAANN program under grant P200A060071, and R. G. P. by the Ohio Research Scholars Program.

[1] J. X. Wang, I. K. Robinson, B. M. Ocko, and R. R. Adzic, *J. Phys. Chem. B* **109**, 24 (2005).
 [2] N. Katsonis, E. Lacaze, and B. L. Feringa, *J. Mater. Chem.* **18**, 2065 (2008).
 [3] D. R. Link, G. Natale, R. Shao, J. E. Maclennan, N. A. Clark, E. Körblova, and D. M. Walba, *Science* **278**, 1924 (1997).
 [4] H. Jaganathan, J. M. Kinsella, and A. Ivanisevic, *Chem. Phys. Chem.* **9**, 2203 (2008).
 [5] S. Jiang and M. Liu, *J. Phys. Chem. B* **108**, 2880 (2004).
 [6] N. Kanda, K. Konishi, and M. Kuwaka-Gonokami, *Opt. Express* **15**, 11 117 (2007).
 [7] L. Z. Liu, X. L. Wu, Z. Y. Zhang, T. H. Li, and P. K. Chu, *Appl. Phys. Lett.* **94**, 253110 (2009).
 [8] K. Robbie, M. J. Brett, and A. Lakhtakia, *Nature (London)* **384**, 616 (1996).

[9] Y. Choi, T. J. Atherton, S. Ferjani, R. G. Petschek, and C. Rosenblatt, *Phys. Rev. E* **80**, 060701(R) (2009).
 [10] J. V. Selinger, Z.-G. Wang, R. F. Bruinsma, and C. M. Knobler, *Phys. Rev. Lett.* **70**, 1139 (1993).
 [11] J. Maclennan and M. Seul, *Phys. Rev. Lett.* **69**, 2082 (1992).
 [12] A. L. Alexe-Ionescu, G. Barbero, and I. Lelidis, *Phys. Rev. E* **66**, 061705 (2002).
 [13] O. D. Lavrentovich and V. M. Pergamenschchik, *Int. J. Mod. Phys. B* **9**, 2389 (1995).
 [14] S. Faetti, *Phys. Rev. E* **49**, 4192 (1994).
 [15] D. Schmidt, E. Schubert, and M. Schubert, *Phys. Status Solidi B* **205**, 748 (2008).
 [16] L. Cao, S. F. Y. Li, and X. C. Zhou, *Analyst (Amsterdam)* **126**, 184 (2001).
 [17] S. Garoff and R. B. Meyer, *Phys. Rev. Lett.* **38**, 848 (1977).
 [18] Z. Li, R. G. Petschek, and C. Rosenblatt, *Phys. Rev. Lett.* **62**, 796 (1989).
 [19] Z. Li, G. A. DiLisi, R. G. Petschek, and C. Rosenblatt, *Phys. Rev. A* **41**, 1997 (1990).
 [20] K. Nakagawa, T. Shinomiya, M. Koden, K. Tsubota, T. Kuratate, Y. Ishii, F. Funada, M. Matura, and K. Awane, *Ferroelectrics* **85**, 39 (1988).
 [21] J.-Z. Xue and N. A. Clark, *Phys. Rev. Lett.* **64**, 307 (1990).
 [22] S.-D. Lee, J. S. Patel, and J. W. Goodby, *Phys. Rev. A* **44**, 2749 (1991).
 [23] M. Kimura, Y. Yamada, H. Ishihara, and T. Akahane, *Mol. Cryst. Liq. Cryst. Sci. Technol., Sect. A* **302**, 199 (1997).
 [24] L. Komitov, B. Helgee, J. Felix, and A. Matharu, *Appl. Phys. Lett.* **86**, 023502 (2005).
 [25] M. Skarabot, I. Musevic, B. Helgee, and L. Komitov, *J. Appl. Phys.* **98**, 046109 (2005).
 [26] S. Tripathi, M.-H. Lu, E. M. Terentjev, R. G. Petschek, and C. Rosenblatt, *Phys. Rev. Lett.* **67**, 3400 (1991).
 [27] D. Harrison, M. R. Fisch, R. G. Petschek, J.-F. Li, F. Harris, and H. Korns, *Jpn. J. Appl. Phys.* **41**, 2183 (2002).
 [28] M. Nakata, G. Zanchetta, M. Buscaglia, T. Bellini, and N. A. Clark, *Langmuir* **24**, 10390 (2008).
 [29] P. G. DeGennes and J. Prost, *Physics of Liquid Crystals* (Clarendon, Oxford, 1994).
 [30] A. Rapini and M. Papoular, *J. Phys. (Paris), Colloq.* **30**, C4-54 (1969).
 [31] A. DeLuca, V. Barna, T. J. Atherton, G. Carbone, M. E. Sousa, and C. Rosenblatt, *Nature Phys.* **4**, 869 (2008).
 [32] V. Barna, A. De Luca, and C. Rosenblatt, *Nanotechnology* **19**, 325709 (2008).
 [33] I. Kobayashi (private communication), based on manufacturer’s specifications.
 [34] I. Syed, G. Carbone, and C. Rosenblatt, *J. Appl. Phys.* **98**, 034303 (2005).
 [35] N. A. Clark, *Phys. Rev. Lett.* **55**, 292 (1985).
 [36] G. Barbero, I. Dozov, J. F. Paliarne, and G. Durand, *Phys. Rev. Lett.* **56**, 2056 (1986).
 [37] V. G. Nazarenko, R. Klouda, and O. D. Lavrentovich, *Phys. Rev. E* **57**, R36 (1998).
 [38] D. Kang and C. Rosenblatt, *Phys. Rev. E* **53**, 2976 (1996).
 [39] J.-H. Kim, M. Yoneya, and H. Yokoyama, U.S. Patent No. 7 342 628 (2008).
 [40] H. Yokoyama (private communication).